



Lawrence Berkeley Laboratory

UNIVERSITY OF CALIFORNIA

Physics, Computer Science & Mathematics Division

Submitted to Physical Review Letters

RECEIVED
LAWRENCE
BERKELEY LABORATORY

DEC 3 1980

POLARIZATION OF MUOPRODUCED $J/\psi(3100)$

LIBRARY AND
DOCUMENTS SECTION

A.R. Clark, K.J. Johnson, L.T. Kerth, S.C. Loken, T.W. Markiewicz,
P.D. Meyers, W.H. Smith, M. Strovink, W.A. Wenzel, R.P. Johnson,
C. Moore, M. Mugge, R.E. Shafer, G.D. Gollin, F.C. Shoemaker,
and P. Surko

October 1980



LBL-11562-C2

DISCLAIMER

This document was prepared as an account of work sponsored by the United States Government. While this document is believed to contain correct information, neither the United States Government nor any agency thereof, nor the Regents of the University of California, nor any of their employees, makes any warranty, express or implied, or assumes any legal responsibility for the accuracy, completeness, or usefulness of any information, apparatus, product, or process disclosed, or represents that its use would not infringe privately owned rights. Reference herein to any specific commercial product, process, or service by its trade name, trademark, manufacturer, or otherwise, does not necessarily constitute or imply its endorsement, recommendation, or favoring by the United States Government or any agency thereof, or the Regents of the University of California. The views and opinions of authors expressed herein do not necessarily state or reflect those of the United States Government or any agency thereof or the Regents of the University of California.

Polarization of Muoproduced $J/\psi(3100)$

A.R. Clark, K.J. Johnson, L.T. Kerth, S.C. Loken, T.W. Markiewicz,

P.D. Meyers, W.H. Smith, M. Strovink, and W.A. Wenzel

Physics Department and Lawrence Berkeley Laboratory,
University of California, Berkeley, California 94720

and

R.P. Johnson, C. Moore, M. Mugge, and R.E. Shafer

Fermi National Accelerator Laboratory,
Batavia, Illinois 60510

and

G.D. Gollin^a, F.C. Shoemaker, and P. Surko^b

Joseph Henry Laboratories, Princeton University,
Princeton, New Jersey 08544

We have analyzed the polarization and Q^2 -dependence of muoproduced $\psi \rightarrow \mu^+ \mu^-$ in a magnetized-steel calorimeter at Fermilab. The reaction $\gamma_V N \rightarrow \psi N$ is found to be helicity-conserving. Even allowing for possible Q^2 -dependence of the decay angular distribution, the ψ muoproduction cross section falls more steeply in Q^2 than predicted by ψ dominance.

We have measured the polarization of $J/\psi(3100)$ produced by 209-GeV muons, analyzed by the decay $\psi \rightarrow \mu^+ \mu^-$. These are the first data on the polarization of any charmonium state produced by real or virtual photon-nucleon collisions. Measurement of the ψ polarization is an essential component of the study of ψ -leptoproduction mechanisms, which was begun¹ with a subset of these data. If ψ -N elastic scattering is helicity-conserving, the polarization of elastically leptoproduced ψ 's in the vector-meson-dominance (VMD) picture² is simply related to that of the exchanged photon. In this case, the data measure R , the ratio σ_L/σ_T of ψ production cross sections by longitudinally and transversely polarized virtual photons (γ_L and γ_T). Since R must vanish at $Q^2=0$, it is a function of Q^2 which must be incorporated in any complete description of the Q^2 -dependence of ψ leptoproduction.

The magnetized-iron multimMuon spectrometer and ψ reconstruction analysis have been described¹. With a slightly different analysis, the dimuon mass spectrum of $\approx 10^6$ trimuon final states (75% of the data) has been published³. The present 2500-event (ψ and ψ') sample, based on the same data, is more tightly cut. The sample is characterized as elastically produced, with events depositing less than (4.5 ± 2.5) GeV in the calorimeter. The real and Monte Carlo (MC) simulated widths of the ψ mass peak are 8.8% and 8.3% rms, respectively. After the production mechanisms in the simulation are adjusted to yield detailed agreement with the data, the calculated average efficiency for detection and analysis of ψ 's elastically produced within the fiducial target is 21%.

The angular distributions of the decay products of electroproduced lower-mass vector mesons⁴ have shown the production process to be consistent with s-channel helicity conservation (SCHC) and natural parity exchange (NPE). With these assumptions, the distribution of dimuons from ψ decay is⁵

$$W(\eta, R; \theta, \phi) = [3/16\pi (1+\epsilon R)] \{1 + \cos^2\theta + \epsilon (2R - \eta \cos 2\phi) \sin^2\theta + F \sin 2\theta\}.$$

Here θ is the polar angle of the beam-sign daughter muon in the ψ rest frame, with $\theta=\pi$ taken as the direction of target recoil. The azimuthal "polarization angle" in this "helicity frame" is $\phi = \cos^{-1}(\hat{n}_d \cdot \hat{n}_p) - \cos^{-1}(\hat{n}_p \cdot \hat{n}_s)$, where \hat{n}_s , \hat{n}_p , and \hat{n}_d are the unit normals to the incident muon scattering, ψ photoproduction, and ψ decay planes, respectively. We use ϵ to denote the ratio of γ_L to γ_T fluxes, and introduce the factor η to monitor the size of the $\cos 2\phi$ term: $\eta=1$ if SCHC and NPE are exactly obeyed. The function F , arising from the single spin flip elements of the density matrix, is

$$F = \sqrt{2\epsilon R} \sin 2\theta \{ \sqrt{1+\epsilon} \cos \delta \cos \psi - H \sqrt{1-\epsilon} \sin \delta \sin \psi \},$$

where H is the muon polarization and δ is the phase difference between amplitudes for ψ production by γ_L and γ_T . This term produces effects too small to be observed in these data.

To avoid statistical problems with low bin populations we have folded θ and ϕ into one quadrant, eliminating any sensitivity of W to F . The data were divided into a $4 \times 5 \times 3$ grid in Q^2 , $|\cos \theta|$, and $\phi_F \equiv \frac{1}{2} \cos^{-1} |\cos 2\phi|$; dimuon-mass-continuum subtractions were performed in each of the 60 bins to obtain the acceptance-corrected ψ yields displayed in Table 1. Unfolding resolution effects by using the average values of Q^2 , ϵ , $\cos^2\theta$, and $\cos 2\phi$ from the MC simulation for each bin, these yields were fit to the product of $W(\eta, R)$ and the propagator $P(\Lambda) \equiv (1 + Q^2/\Lambda^2)^{-2}$. Thereby, allowance was made for the possibility that the decay angular distribution is a function of Q^2 through the Q^2 -dependence of R , e.g. $R \propto Q^2/m_\psi^2$ as suggested² by VMD. Since the experimental acceptance is not uniform in $\cos \theta$, such a dependence could have biased our measurement of Λ if the data had been summed over all angles.

The details of the fits are presented in Table 2. Three-parameter fits to

η , R , and Λ are made both with $R \propto Q^2$ (fits 1 and 6) and with $R = \text{constant}$ over the Q^2 range (fit 2). The parameter Λ describes the Q^2 -dependence of the effective sum $\sigma_{\text{eff}} = \sigma_T + \epsilon \sigma_L$ of γ_T and γ_L cross sections, or, in the case of fit 6, only of σ_T . An additional complication is the possible Q^2 -dependence of any nuclear shadowing in the Fe target. We have used data which recently were summarized⁶ for $A \approx 200$, scaled the data to $A = 56$, and fit a universal curve in $x' \equiv Q^2 / (2m_N \nu + m_N^2)$:

$$\Lambda_{\text{eff}} / \Lambda(\text{Fe}) \equiv S(x') = (1 - 0.33 \exp(-28x'))^{0.76}.$$

All fits are made both with and without $S(x')$ multiplying W . As the results in Table 2 indicate, including $S(x')$ lowers the propagator mass Λ , but hardly affects the angular results.

The results of fits 1-4 are shown in Fig. 1. For purposes of this display only, the data and fits plotted vs. $|\cos\theta|$ (ϕ_F) are summed over ϕ_F ($|\cos\theta|$). The main feature of these angular distributions is a strong dependence upon ϕ_F , in the form predicted by SCHC. Unpolarized ψ 's would yield a flat angular distribution (fit 3), which is ruled out. The data show no strong dependence on $|\cos\theta|$, but do not rule out $R=0$ (fit 4); significant Q^2 -dependence of R is not required (fit 2). The photon-gluon-fusion (γGF) model⁷, which has successfully described⁸ other features of elastic ψ muoproduction, has yielded no prediction for the ψ polarization. This is due in part to complications associated with the exchange, required by color conservation, of at least two vector gluons.

Figure 2 presents the Q^2 -dependence of σ_{eff} , summed over ν and normalized to unity at $Q^2=0$. For purposes of this display only, the data and fits to Λ are summed over $|\cos\theta|$ and ϕ_F . When the angular distribution is parameterized in the SCHC form with $R \propto Q^2$ and $S(x')$ included, $\Lambda = 2.03^{+0.18}_{-0.12} \text{ GeV}/c^2$, where the sta-

tistical errors take into account the uncertainties in η and ξ^2 (Table 2, fit 1). If instead $R=\text{constant}$ and $S(x')$ is left out, $\Lambda=2.43\pm0.15$ GeV/c² (fit 2). The other fits to Λ , either for σ_{eff} or σ_T (fit 6), are within this 2.0-2.4 GeV/c² range; this ±0.2 GeV/c² uncertainty is the principal systematic error in Λ . We conclude that Λ is between 1.9 and 2.6 GeV/c². The simplest VMD prediction, $\Lambda=m_\psi$ (fit 5), is ruled out.

We also have fit the data in Fig. 2 to the γGF prediction (fit 7), assuming a charmed quark mass $m_c=1.5$ GeV/c² and a gluon fractional-momentum distribution $G(x)=3(1-x)^5/x$. The data fall faster than the γGF curve, giving a barely acceptable fit (7% confidence) only if $S(x')$ is omitted. We have reached a similar conclusion⁹ comparing γGF predictions with open-charm muoproduction, using a different analysis. Varying m_c , the exponent of $(1-x)$ in $G(x)$, or the definition of the strong coupling constant can affect the γGF fit. A combined determination of these parameters must be based on both the Q^2 and ν spectra of the ψ data.

In summary, the polar and azimuthal angle distributions for muoproduced $\psi \rightarrow \mu^+ \mu^-$ decay demonstrate that the reaction $\gamma_V N \rightarrow \psi N$ is consistent with g -channel helicity conservation and natural parity exchange. There is some indication of longitudinally polarized production ($R \neq 0$). The Q^2 -dependence of either σ_{eff} or σ_T clearly is steeper than $(1+Q^2/m_\psi^2)^{-2}$.

This work was supported by the High Energy Physics Division of the U.S. Department of Energy under Contract Nos. W-7405-Eng-48, DE-AC02-76ER03072, and EY-76-C-02-3000.

References

- ^aNow at Enrico Fermi Institute, Chicago, Illinois 60637.
- ^bNow at Bell Laboratories, Murray Hill, New Jersey 07974.
- ¹A.R. Clark et al., Phys. Rev. Lett. 43, 187 (1979).
- ²J.J. Sakurai and D. Schildknecht, Phys. Lett. 40B, 121 (1972).
- ³A.R. Clark et al., Phys. Rev. Lett. 45, 686 (1980).
- ⁴J.T. Dakin et al., Phys. Rev. Lett. 30, 142 (1972); W.R. Francis et al., Phys. Rev. Lett. 38, 633 (1977); R. Dixon et al., Phys. Rev. Lett. 39, 516 (1977).
- ⁵K. Schilling, P. Seyboth, and G. Wolf, Nuc. Phys. B15, 397 (1970); B. Humpert and A.C.D. Wright, Ann. Phys. 110, 1 (1978); T. Markiewicz, Ph.D. Thesis, Univ. of Calif., Berkeley, 1980 (unpublished).
- ⁶H. Miettinen, presented at the XX International Conference on High Energy Physics, Madison, Wisconsin, July 17-23, 1980.
- ⁷J.T. Leveille and T. Weiler, Phys. Rev. D20, 630 (1979), and references cited therein.
- ⁸T. Weiler, Phys. Rev. Lett. 44, 301 (1980); V. Barger, W.Y. Keung, and R.J.N. Phillips, Phys. Lett. 91B, 253 (1980).
- ⁹A.R. Clark et al., Phys. Rev. Lett. 45, 1465 (1980).

TABLE 1. Effective cross section, differential in $\cos\theta$ and ϕ , for the reaction $\gamma_V \text{Fe} \rightarrow \psi X$ (energy(X) < 4.5 GeV), in arbitrary units. Data and statistical errors are given in 60 bins, defined by average Q^2 (top row), average $\cos^2\theta$ (left column), and one of three ϕ bins (second-left column). The average $\cos 2\phi$ in each ϕ bin is given vs. $\langle Q^2 \rangle$ in the bottom three rows; values of average ϵ are in the right column. At lowest Q^2 , average $\cos 2\phi$ in ϕ bin 1 (2) grows by 0.32 (0.23) as $\cos^2\theta$ rises from 0.02 to 0.54. The variation of average $\cos 2\phi$ with $\cos^2\theta$ is much weaker in other bins, and negligible at highest Q^2 .

$\langle Q^2 \rangle (\text{GeV}/c)^2$		0.10	0.53	1.60	6.34		
$\cos^2\theta$	ϕ bin	$d^2\sigma(\text{eff})/d\phi d\cos\theta$ (arbitrary units)				$\langle \epsilon \rangle$	
0.02	1	0.52(07)	0.37(09)	0.30(10)	0.05(07)	0.82	
	2	0.55(07)	0.61(11)	0.36(11)	0.10(05)		
	3	0.59(06)	0.64(13)	0.44(09)	0.35(11)		
0.06	1	0.51(06)	0.24(07)	0.36(13)	0.05(04)	0.81	
	2	0.61(07)	0.68(13)	0.35(10)	0.27(10)		
	3	0.50(06)	0.76(14)	0.54(11)	0.22(06)		
0.16	1	0.54(07)	0.25(11)	0.22(10)	0.04(05)	0.80	
	2	0.64(08)	0.52(12)	0.36(11)	0.09(04)		
	3	0.52(07)	0.56(11)	0.49(11)	0.11(05)		
0.32	1	0.58(08)	0.32(12)	0.36(13)	0.04(06)	0.76	
	2	0.46(08)	0.47(16)	0.27(09)	0.12(07)		
	3	0.62(09)	0.66(14)	0.39(10)	0.11(06)		
0.54	1	0.55(28)	0.91(34)	0.31(25)	0.12(10)	0.65	
	2	0.67(20)	0.15(28)	0.48(22)	0.05(10)		
	3	1.09(29)	1.21(48)	0.35(28)	0.12(10)		
$\cos 2\phi$	1	-0.09	0.54	0.73	0.80		
	2	-0.26	-0.11	-0.07	-0.03		
	3	-0.46	-0.72	-0.74	-0.81		

TABLE 2. Fits to the Q^2 , ϕ , and θ -dependence of the effective cross section σ_{eff} for the reaction $\gamma_V \text{Fe} \rightarrow \psi X$ (energy(X) < 4.5 GeV). The angular function $W(\eta, R)$, propagator $P(\Lambda)$, and nuclear screening factor $S(x')$ are defined in the text. Each of seven fits (numbered in the first column) is performed both with $S(x')$ included (multiplied "in") and ignored ("out") in the function fitted. Values of chi-squared and the degrees of freedom are given in the fourth column. Errors on the fit parameters Λ , η , and ξ^2 (fits 1 and 6) or R (fit 2) are statistical. Fit 6 is the same as fit 1 except that W is multiplied by $(1+\epsilon R)$; Λ then parameterizes the Q^2 -dependence of σ_T rather than σ_{eff} . Fit 7 compares the data integrated over ϕ and $\cos\theta$ with the Q^2 -dependence predicted by γGF .

Fit No.	Function	$S(x')$	χ^2/DF	$\Lambda(\text{GeV}/c^2)$	η	ξ^2 or R
1	$W(\eta, R) \times P(\Lambda)$ $R = (\xi Q/m_\psi)^2$	in	45.4/56	$2.03^{+0.18}_{-0.12}$	$1.02^{+0.28}_{-0.23}$	$3.3^{+4.9}_{-3.0}$
		out	45.5/56	$2.18^{+0.18}_{-0.13}$	$1.04^{+0.28}_{-0.23}$	$4.0^{+4.8}_{-3.4}$
2	$W(\eta, R) \times P(\Lambda)$ $R = \text{constant}$	in	42.0/56	2.24 ± 0.13	$1.09^{+0.31}_{-0.24}$	$.35^{+.26}_{- .18}$
		out	42.4/56	2.43 ± 0.15	$1.10^{+0.31}_{-0.24}$	$.37^{+.27}_{- .22}$
3	$1 \times P(\Lambda)$	in	73.3/58	2.06 ± 0.11		
		out	73.3/58	2.22 ± 0.13		
4	$W(1, 0) \times P(\Lambda)$	in	48.6/58	2.21 ± 0.12	$\equiv 1$	$\equiv 0$
		out	49.3/58	2.40 ± 0.14		
5	$W(\eta, 0) \times P(m_\psi)$	in	89.1/58	$\equiv 3.1$	0.96 ± 0.13	$\equiv 0$
		out	68.5/58		0.93 ± 0.14	
6	$(1+\epsilon R) \times \text{Fit 1}$	in	47.0/56	2.08 ± 0.24	0.86 ± 0.17	$.24^{+.61}_{- .39}$
		out	47.6/56	2.20 ± 0.29	0.87 ± 0.17	$.34^{+.75}_{- .43}$
7	$\gamma\text{GF} \text{ -- } Q^2$ projection	in	32.1/8	$m_c \equiv 1.5 \text{ GeV}/c^2$		
		out	14.6/8			

Figure Captions

FIG. 1. Angular dependence of the effective cross section for the reaction $\gamma_V \text{Fe} \rightarrow \psi X$ (energy(X) < 4.5 GeV). Data and statistical errors are presented vs. $|\cos\theta|$ (left column) and ϕ_F (right column), where ϕ_F is ϕ folded into one quadrant; θ and ϕ are defined in the text. All data ($\langle Q^2 \rangle = 0.71$) are shown in (a); (b)-(e) divide the data into four Q^2 regions. Numbered solid lines exhibit the results of fits 1-4 in Table 2. Fits 1, 2, and 4 are to the SCHC formula with $\sigma_L/\sigma_T = \xi^2 Q^2/m_\psi^2$, constant, and zero, respectively; fit 3 corresponds to the production of unpolarized ψ 's. Each fit is made to all the data with one adjustable normalization constant.

FIG. 2. Q^2 -dependence of the effective cross section for the reaction $\gamma_V \text{Fe} \rightarrow \psi X$ (energy(X) < 4.5 GeV). Statistical errors are shown. Typical Q^2 resolution is 3.1 (0.6) (GeV/c) 2 at $Q^2 = 17$ (1.2) (GeV/c) 2 . The data are fit to $(1+Q^2/\Lambda^2)^{-2}$ multiplied by the function $W(\eta, R)$ shown in Table 2. The weak Q^2 -dependence of W results from the Q^2 -dependence of $R = \sigma_L/\sigma_T$ and the particular average values of the angular factors $\cos^2\theta$ and $\cos 2\phi$, as given in Table 1. The best fits with free Λ (Table 2, fit 1) and fixed $\Lambda = 3.1$ (Table 2, fit 5) are shown. The data are normalized so that fit 1 is unity at $Q^2 = 0$. Also exhibited is the γ GF prediction (Table 2, fit 7). At high Q^2 , fits 1 and 7 are displayed as a solid band, with the upper (lower) edge including (omitting) the screening factor $S(x')$.

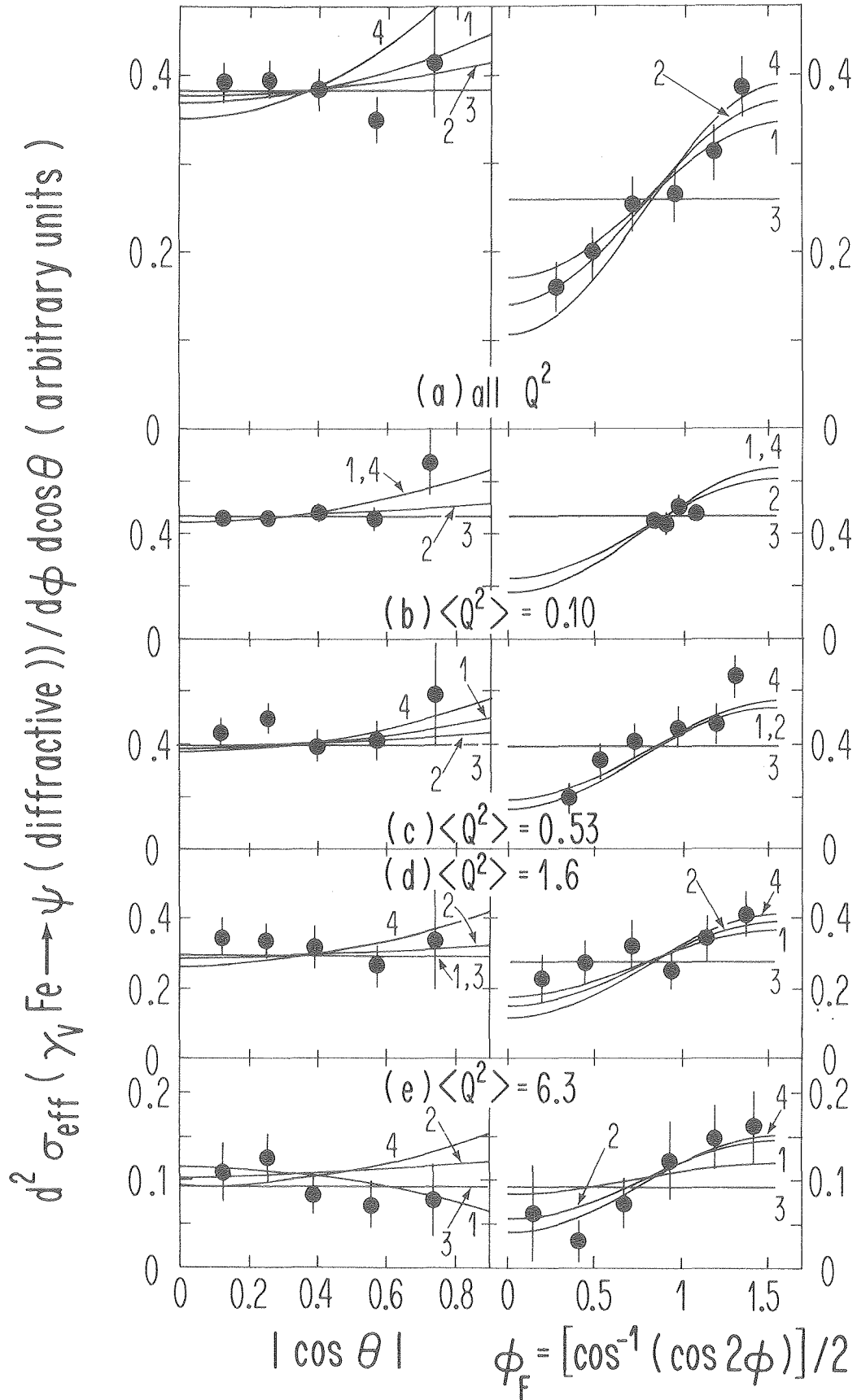


Fig. 1

XBL 809-1801

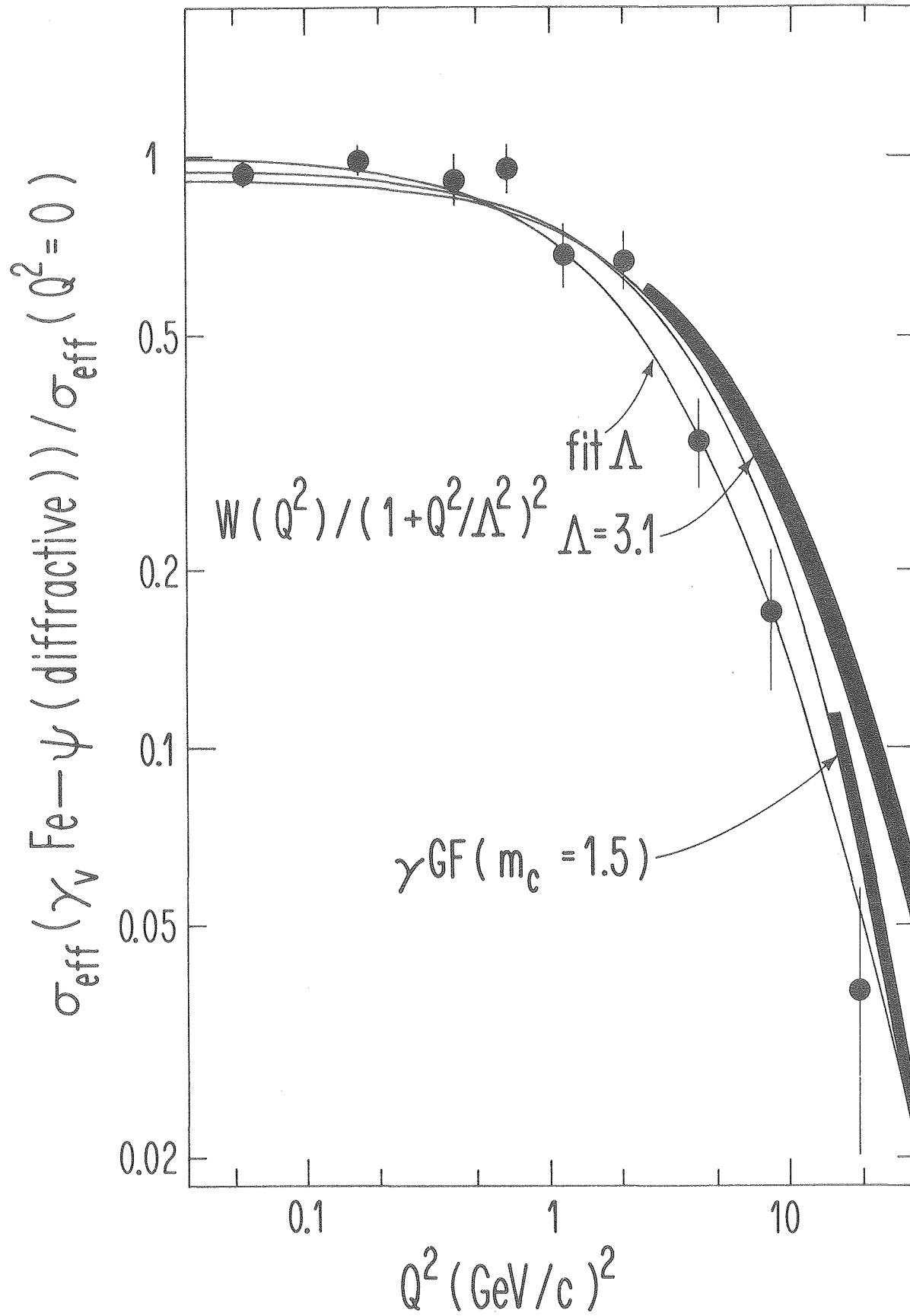


Fig. 2

XBL 808-1800